Cell Metabolism, Volume *37*

Supplemental information

Maternal circadian rhythms during pregnancy dictate metabolic plasticity in offspring

Na Yao, Kenichiro Kinouchi, Manami Katoh, Kousha Changizi Ashtiani, Sherif Abdelkarim, Hiroyuki Morimoto, Takuto Torimitsu, Takahide Kozuma, Akihide Iwahara, Shotaro Kosugi, Jin Komuro, Kyosuke Kato, Shun Tonomura, Toshifumi Nakamura, Arata Itoh, Shintaro Yamaguchi, Jun Yoshino, Junichiro Irie, Hisayuki Hashimoto, Shinsuke Yuasa, Akiko Satoh, Yohei Mikami, Shusaku Uchida, Takatoshi Ueki, Seitaro Nomura, Pierre Baldi, Kaori Hayashi, and Hiroshi Itoh

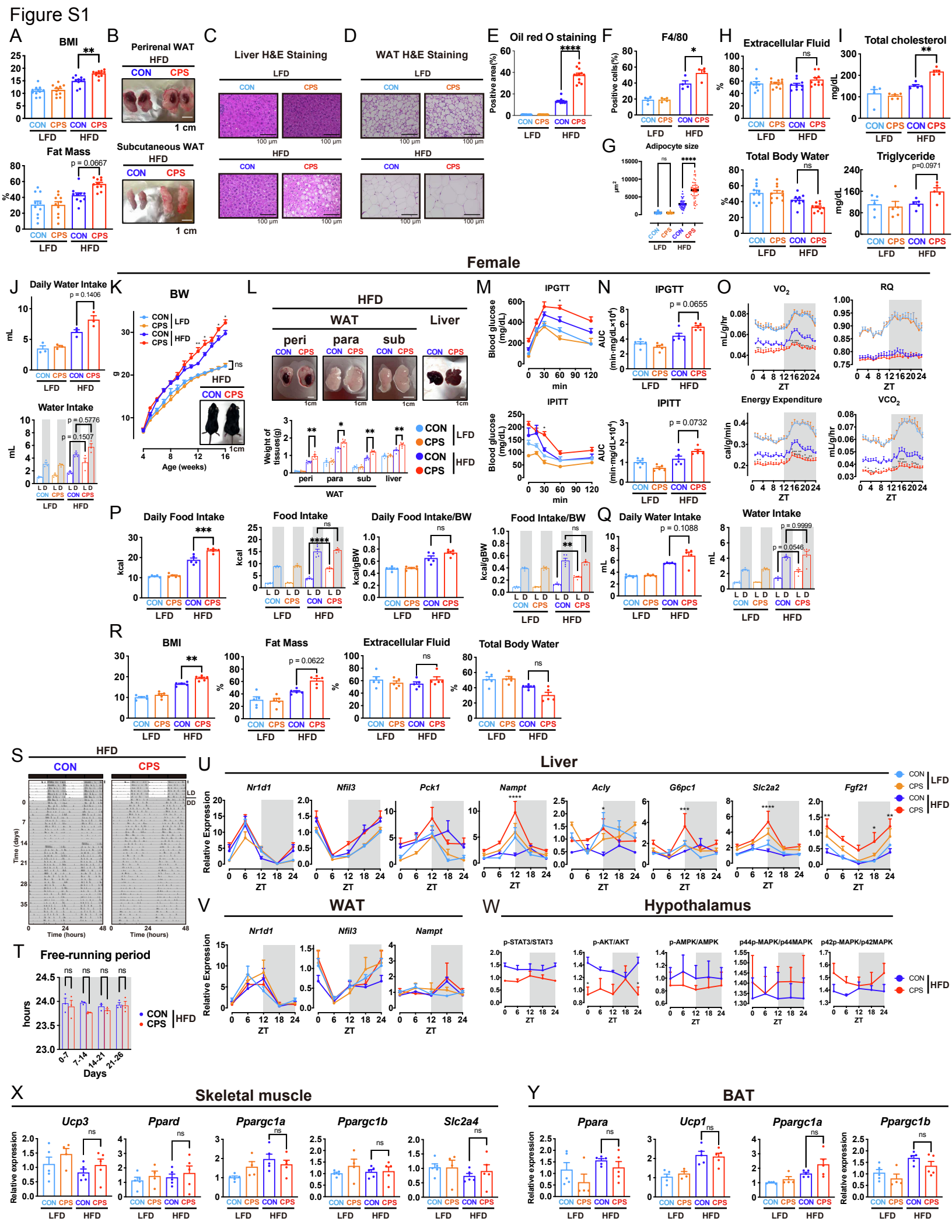
Figure S1
A
BMI
Fat Mass
p = 0.0667
B
Perirenal WAT
HFD
CON CPS
1 cm
Subcutaneous WAT
C
Liver H&E Staining
LFD
HFD
D
WAT H&E Staining
E
Oil red O staining
Positive area(%)
F
F4/80
Positive cells(%)
G
Adipocyte size
H
Extracellular Fluid
Total Body Water
I
Total cholesterol
Triglyceride
p=0.0971
Female
J
Daily Water Intake
p = 0.1406
Water Intake
p = 0.5776
p = 0.1507
K
BW
Age (weeks)
L
HFD
WAT
Liver
peri para sub
Weight of tissues(g)
M
IPGTT
Blood glucose (mg/dL)
min
IPITT
N
IPGTT
AUC
p = 0.0655
IPITT
p = 0.0732
O
VO2
RQ
Energy Expenditure
VCO2
ZT
P
Daily Food Intake
Food Intake
Daily Food Intake/BW
Food Intake/BW
Q
Daily Water Intake
p = 0.1088
Water Intake
p = 0.9999
p = 0.0546
R
BMI
Fat Mass
p = 0.0622
Extracellular Fluid
Total Body Water
S
HFD
CON
CPS
LD
DD
Time (days)
Time (hours)
T
Free-running period
hours
Days
0-7
7-14
14-21
21-28
U
Liver
Nr1d1
Nfil3
Pck1
Nampt
Acly
G6pc1
Slc2a2
Fgf21
Relative Expression
V
WAT
W
Hypothalamus
p-STAT3/STAT3
p-AKT/AKT
p-AMPK/AMPK
p44p-MAPK/p44MAPK
p42p-MAPK/p42MAPK
X
Skeletal muscle
Ucp3
Ppard
Ppargc1a
Ppargc1b
Slc2a4
Relative expression
Y
BAT
Ppara
Ucp1
Ppargc1a
Ppargc1b
CON
CPS
LFD
HFD
ns

Figure S2

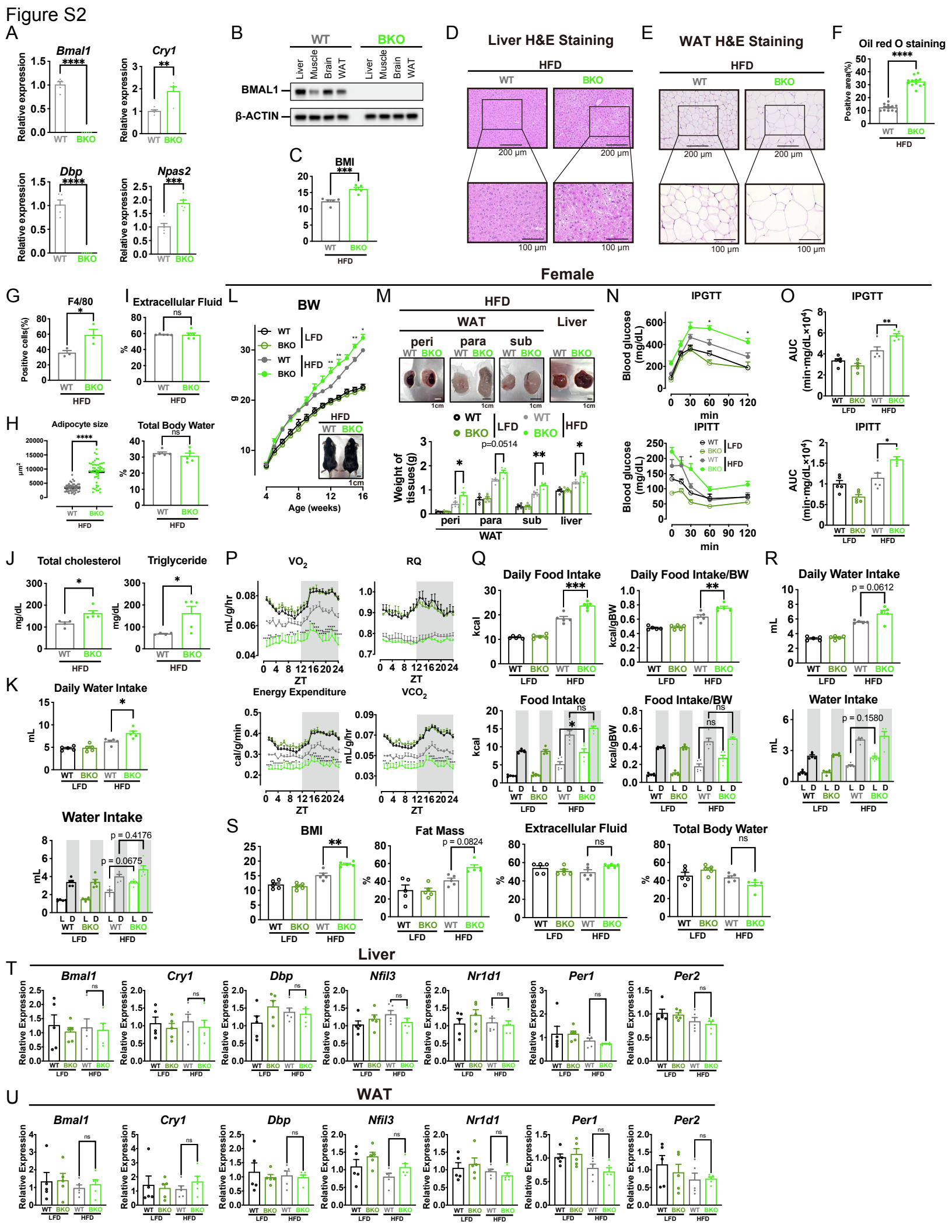
A
Bmal1
Cry1
Dbp
Npas2
Relative expression
WT BKO
B
WT BKO
Liver Muscle Brain WAT Liver Muscle Brain WAT
BMAL1
β-ACTIN
C
BMI
HFD
D
Liver H&E Staining
HFD
200 μm
100 μm
E
WAT H&E Staining
F
Oil red O staining
Positive area(%)
Female
G
F4/80
Positive cells(%)
I
Extracellular Fluid
H
Adipocyte size
Total Body Water
L
BW
LFD
HFD
Age (weeks)
M
WAT
Liver
peri para sub
Weight of tissues(g)
p=0.0514
N
IPGTT
Blood glucose (mg/dL)
min
IPITT
O
AUC (min·mg/dL×10⁴)
J
Total cholesterol
Triglyceride
mg/dL
K
Daily Water Intake
Water Intake
P
VO2
RQ
Energy Expenditure
VCO2
ZT
Q
Daily Food Intake
Daily Food Intake/BW
Food Intake
Food Intake/BW
kcal
kcal/gBW
R
Daily Water Intake
p = 0.0612
Water Intake
p = 0.1580
S
BMI
Fat Mass
p = 0.0824
Extracellular Fluid
Total Body Water
Liver
T
Bmal1 Cry1 Dbp Nfil3 Nr1d1 Per1 Per2
Relative Expression
WAT
U
Bmal1 Cry1 Dbp Nfil3 Nr1d1 Per1 Per2

Figure S3

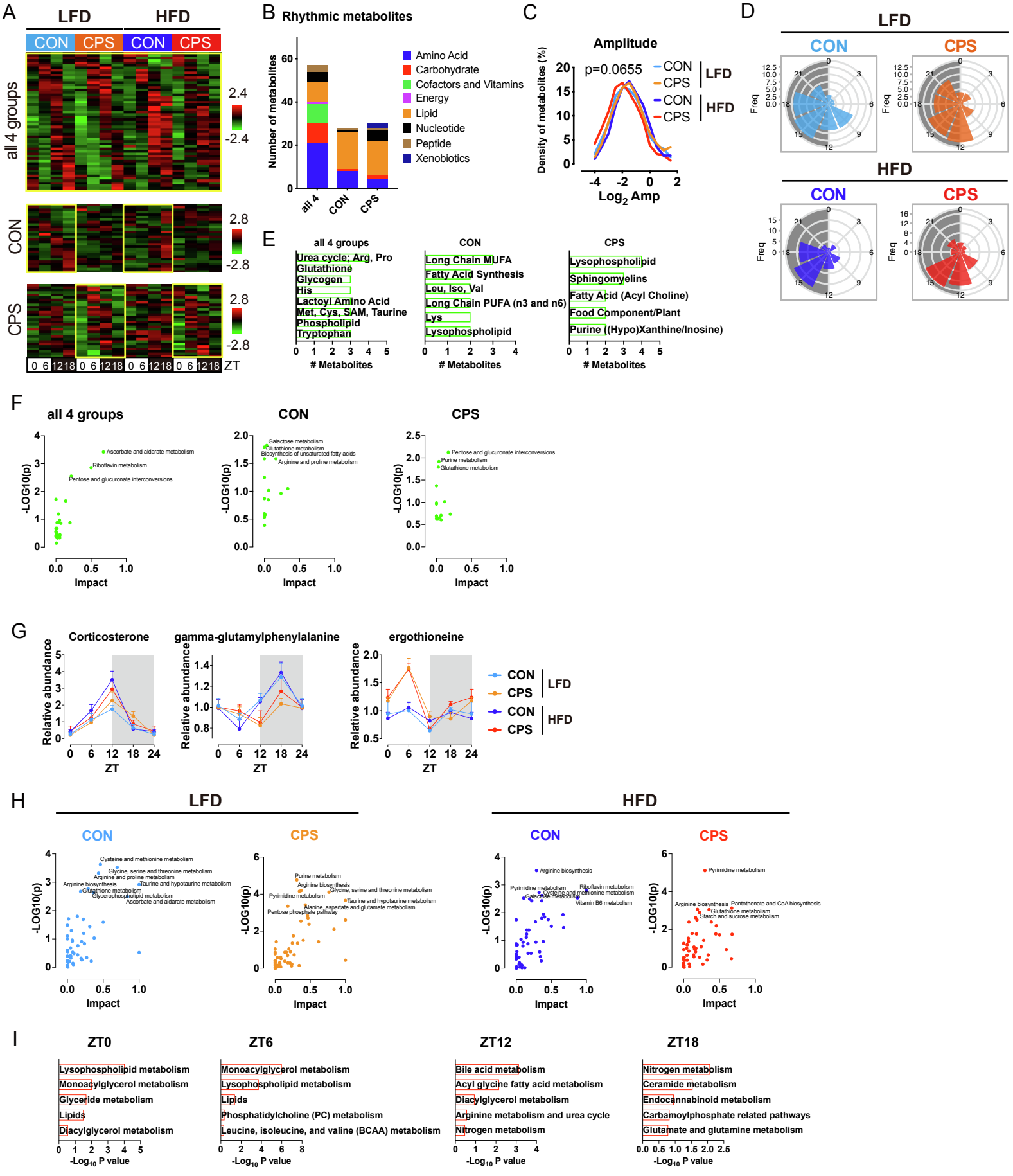
A
LFD
HFD
CON
CPS
CON
CPS
all 4 groups
2.4
-2.4
CON
2.8
-2.8
CPS
2.8
-2.8
0 6 12 18 0 6 12 18 0 6 12 18 0 6 12 18 ZT
B Rhythmic metabolites
Number of metabolites
Amino Acid
Carbohydrate
Cofactors and Vitamins
Energy
Lipid
Nucleotide
Peptide
Xenobiotics
all 4
CON
CPS
C
Amplitude
p=0.0655
CON
CPS
CON
CPS
LFD
HFD
Density of metabolites (%)
Log2 Amp
D
LFD
CON
CPS
HFD
CON
CPS
Freq
E
all 4 groups
Urea cycle; Arg, Pro
Glutathione
Glycogen
His
Lactoyl Amino Acid
Met, Cys, SAM, Taurine
Phospholipid
Tryptophan
Metabolites
CON
Long Chain MUFA
Fatty Acid Synthesis
Leu, Iso, Val
Long Chain PUFA (n3 and n6)
Lys
Lysophospholipid
Metabolites
CPS
Lysophospholipid
Sphingomyelins
Fatty Acid (Acyl Choline)
Food Component/Plant
Purine ((Hypo)Xanthine/Inosine)
Metabolites
F
all 4 groups
Ascorbate and aldarate metabolism
Riboflavin metabolism
Pentose and glucuronate interconversions
-LOG10(p)
Impact
CON
Galactose metabolism
Glutathione metabolism
Biosynthesis of unsaturated fatty acids
Arginine and proline metabolism
-LOG10(p)
Impact
CPS
Pentose and glucuronate interconversions
Purine metabolism
Glutathione metabolism
-LOG10(p)
Impact
G
Corticosterone
gamma-glutamylphenylalanine
ergothioneine
Relative abundance
ZT
CON
CPS
CON
CPS
LFD
HFD
H
LFD
HFD
CON
CPS
CON
CPS
-LOG10(p)
Impact
Cysteine and methionine metabolism
Glycine, serine and threonine metabolism
Arginine and proline metabolism
Arginine biosynthesis
Taurine and hypotaurine metabolism
Glutathione metabolism
Glycerophospholipid metabolism
Ascorbate and aldarate metabolism
Purine metabolism
Arginine biosynthesis
Pyrimidine metabolism
Glycine, serine and threonine metabolism
Taurine and hypotaurine metabolism
Alanine, aspartate and glutamate metabolism
Pentose phosphate pathway
Arginine biosynthesis
Pyrimidine metabolism
Cysteine and methionine metabolism
Galactose metabolism
Riboflavin metabolism
Vitamin B6 metabolism
Pyrimidine metabolism
Arginine biosynthesis
Pantothenate and CoA biosynthesis
Glutathione metabolism
Starch and sucrose metabolism
I
ZT0
Lysophospholipid metabolism
Monoacylglycerol metabolism
Glyceride metabolism
Lipids
Diacylglycerol metabolism
-Log10 P value
ZT6
Monoacylglycerol metabolism
Lysophospholipid metabolism
Lipids
Phosphatidylcholine (PC) metabolism
Leucine, isoleucine, and valine (BCAA) metabolism
-Log10 P value
ZT12
Bile acid metabolism
Acyl glycine fatty acid metabolism
Diacylglycerol metabolism
Arginine metabolism and urea cycle
Nitrogen metabolism
-Log10 P value
ZT18
Nitrogen metabolism
Ceramide metabolism
Endocannabinoid metabolism
Carbamoylphosphate related pathways
Glutamate and glutamine metabolism
-Log10 P value

Figure S4

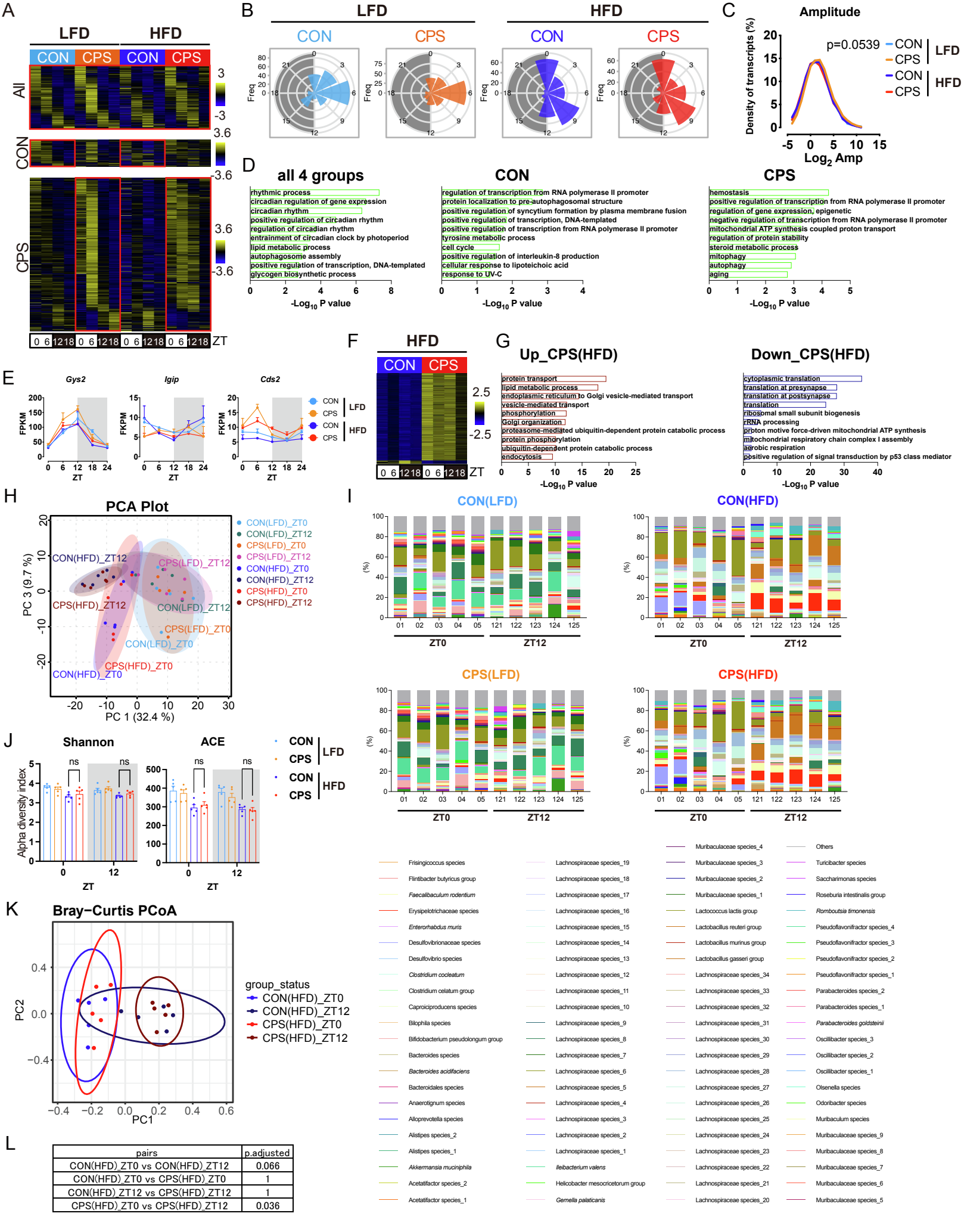

L

pairs	p.adjusted
CON(HFD)_ZT0 vs CON(HFD)_ZT12	0.066
CON(HFD)_ZT0 vs CPS(HFD)_ZT0	1
CON(HFD)_ZT12 vs CPS(HFD)_ZT12	1
CPS(HFD)_ZT0 vs CPS(HFD)_ZT12	0.036

Figure S5

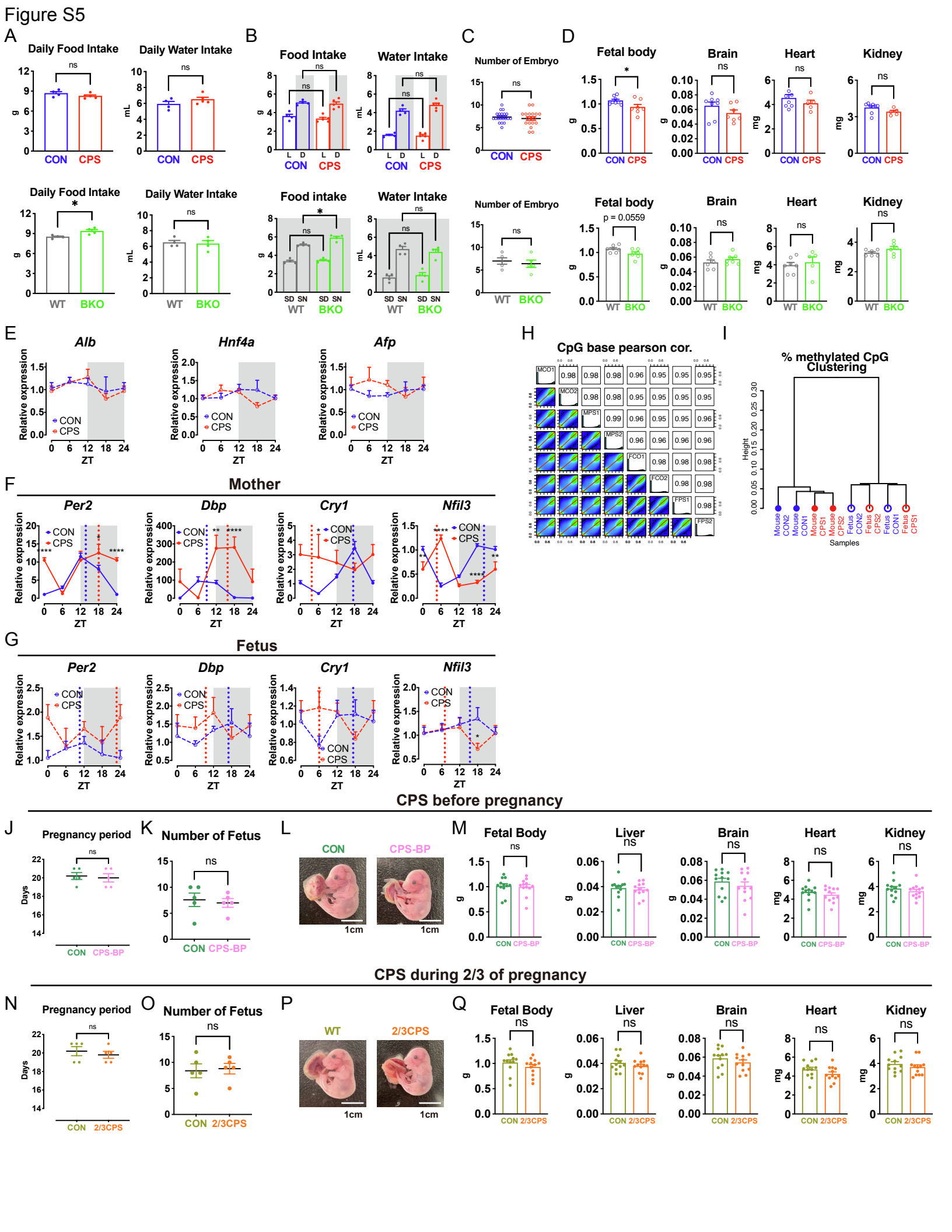
A
Daily Food Intake
Daily Water Intake
CON CPS
WT BKO
B
Food Intake
Water Intake
Food intake
L D
SD SN
C
Number of Embryo
D
Fetal body
Brain
Heart
Kidney
p = 0.0559
E
Alb
Hnf4a
Afp
Relative expression
ZT
H
CpG base pearson cor.
I
% methylated CpG Clustering
Height
Samples
F
Mother
Per2
Dbp
Cry1
Nfil3
G
Fetus
CPS before pregnancy
J
Pregnancy period
Days
K
Number of Fetus
L
CPS-BP
1cm
M
Fetal Body
Liver
CPS during 2/3 of pregnancy
N
O
P
2/3CPS
Q

Figure S6


A
Slc38a4
Cry1
Nfil3
Per2
Nampt
Relative Expression
CON
CPS
ZT
CPS before pregnancy
CPS during 2/3 of pregnancy
B
Placental weight
C
BW/PW
D
Placental Weight
E
BW/PW
ns
g
g/g
CON
CPS-BP
2/3CPS
F
Cell fraction
seurat_clusters
CON1
CON2
CPS1
CPS2
G
H
Meg3
Dtna
Ptprc
Pecam1
Gcm1
Pgf
Dlx3
Tfap2c
Ror2
Tcf7l1
I
Trophoblast-GC (Cluster 0)
Trophoblast-SpT (Cluster 1)
Decidual Stroma (Cluster 3)
Trophoblast-SynT1 (Cluster 4)
Trophoblast-S-TGC (Cluster 6)
Endothelial cells (Cluster 8)
Trophoblast-SynT2 (Cluster 9)
Fetal mesenchyme 3 (Cluster 10)
Blood and immune cells (Cluster 11)
J
Down_endothelial cells
positive regulation of transcription from RNA polymerase II promoter
positive regulation of transcription, DNA-templated
protein phosphorylation
in utero embryonic development
cell migration
phosphorylation
actin cytoskeleton organization
endocytosis
positive regulation of cell migration
-Log10 P value
Up_endothelial cells
cytoplasmic translation
translation
ribosomal small subunit assembly
T cell activation
female pregnancy
ribosomal small subunit biogenesis
phagocytosis
negative regulation of endothelial cell proliferation
ribosomal large subunit assembly
Down_blood and immune cells 1
immune system process
phosphorylation
protein phosphorylation
protein autophosphorylation
positive regulation of GTPase activity
intracellular signal transduction
inflammatory response
endocytosis
positive regulation of interleukin-1 beta production
Up_blood and immune cells 1
cytoplasmic translation
translation
T cell activation
female pregnancy
phagocytosis
positive regulation of lactation
B cell activation
response to nutrient levels
positive regulation of JAK-STAT cascade
Down_blood and immune cells 2
positive regulation of transcription from RNA polymerase II promoter
chromatin organization
endocytosis
phosphorylation
protein phosphorylation
intracellular protein transport
positive regulation of transcription, DNA-templated
negative regulation of transcription, DNA-templated
immune system process
Up_blood and immune cells 2
cytoplasmic translation
translation
female pregnancy
negative regulation of endothelial cell proliferation
positive regulation of lactation
T cell activation
positive regulation of JAK-STAT cascade
phagocytosis
response to nutrient levels

Figure S7

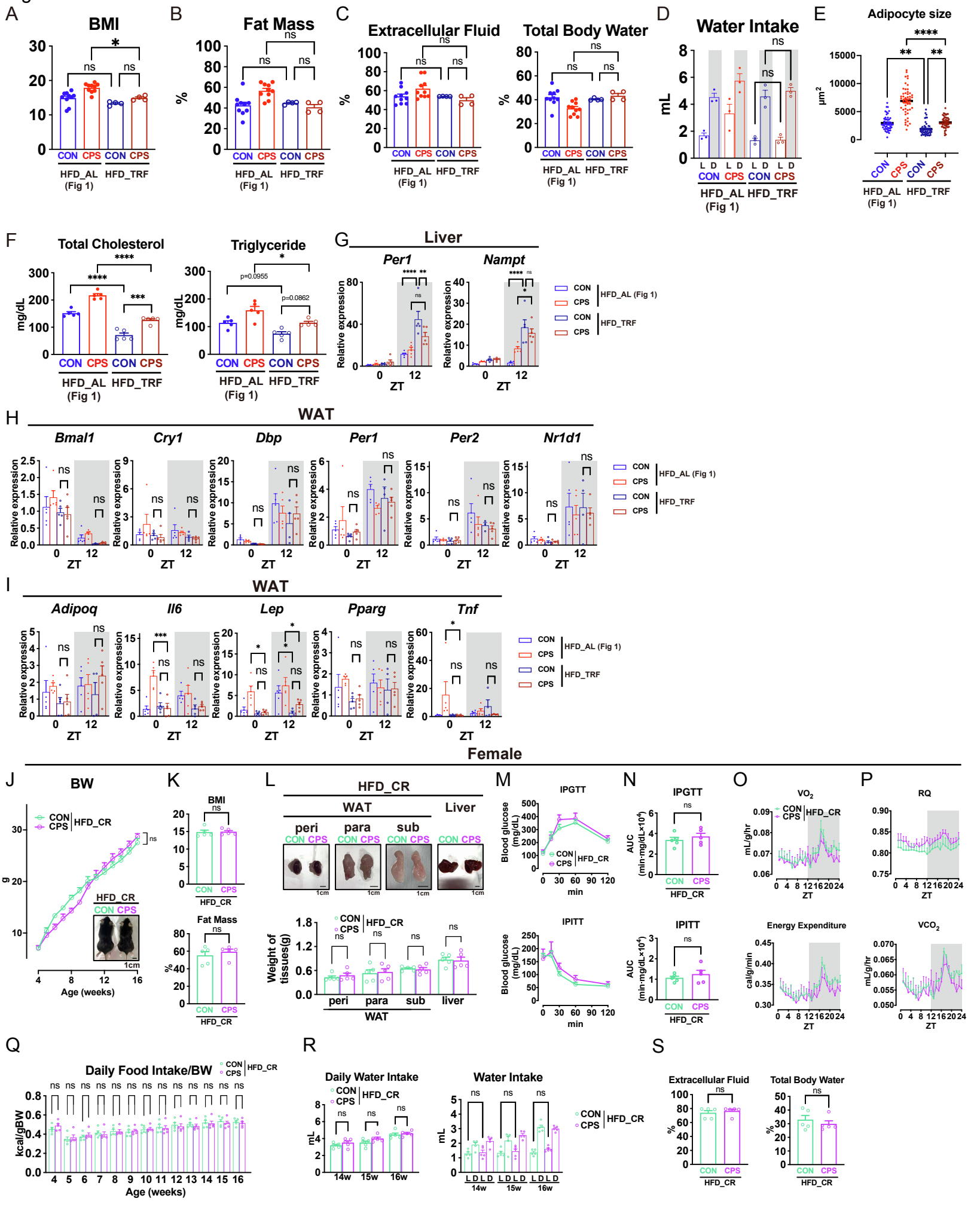
A
BMI
B
Fat Mass
C
Extracellular Fluid
Total Body Water
D
Water Intake
E
Adipocyte size
F
Total Cholesterol
Triglyceride
G
Liver
Per1
Nampt
H
WAT
Bmal1
Cry1
Dbp
Per1
Per2
Nr1d1
I
WAT
Adipoq
Il6
Lep
Pparg
Tnf
CON
CPS
HFD_AL (Fig 1)
HFD_TRF
ZT
Relative expression
Female
J
BW
K
BMI
Fat Mass
L
HFD_CR
WAT
Liver
peri
para
sub
liver
Weight of tissues(g)
M
IPGTT
IPITT
Blood glucose (mg/dL)
min
N
IPGTT
IPITT
AUC
O
VO2
Energy Expenditure
P
RQ
VCO2
Q
Daily Food Intake/BW
kcal/gBW
Age (weeks)
R
Daily Water Intake
Water Intake
S
Extracellular Fluid
Total Body Water

Supplementary Figure Legend

Figure S1. Maternal circadian disruption during pregnancy promotes diet-induced obesity in offspring, related to Figure 1.

(A) Body mass index (BMI, top) and percentage of fat mass (bottom) determined by the bioimpedance method (n=10 animals per group). (B) Representative photographs of perirenal (top) and subcutaneous (bottom) white adipose tissues (WAT). (C, D) Representative images of the liver (C) and WAT H&E staining (D). (E) Percentage of oil red O staining-positive areas shown in Figure 1G (n=3 mice per group, four areas were captured and analyzed in each mouse). (F) Percentage of F4/80 positive cells in the immunohistochemistry staining shown in Figure 1H (n=4 replicates per group). (G) Adipocyte size in H&E staining (areas of 50 cells derived from n=3 replicates per group (17, 17, 16 cells from each replicate) were counted in each group). Data are presented as mean ± SEM. (H) Percentage of extracellular fluid (top) and total body water (bottom) determined by the bioimpedance method (n=10 animals per group). (I) Serum levels of total cholesterol (top) and triglyceride (bottom) (n=5 samples per group). (J) Daily water intake (n=3 animals per group). L, light; D, dark. (K) Body weight of the LFD- or HFD-fed female offspring mice of the CON and CPS mothers (n=5 animals per group). (L) Representative photograph of the WAT and liver from the HFD-fed female offspring mice of the CON and CPS mothers (top), and tissue weights of the LFD- or HFD-fed offspring mice of the CON and CPS mothers (n=5 tissues per group, bottom). peri, perirenal; para, parametrial; sub, subcutaneous. (M) Intraperitoneal glucose (top) and insulin tolerance tests (bottom) (n=5 animals per group). (N) Area under the curve (AUC) of the glucose (top) and insulin tolerance tests (bottom) (n=5 animals per group). (O) Metabolic cage assessment of the oxygen consumption (VO_2), energy expenditure, respiratory quotient (RQ), and carbon dioxide production (VCO_2) (n=4 animals per group) in female offspring mice aged from 14 to 16 weeks. (P) Daily food intake (left panels) and food intake adjusted by body weight (right panels) (n=5 animals per group). L and D denote light and dark phases, respectively. (Q) Daily water intake (n=5 animals per group). L, light; D, dark. (R) Body mass index (BMI), percentage of fat mass, percentage of extracellular fluid and total body water determined using the bioimpedance method (n=5 animals per group). (S) Representative free-running locomotor activities of the HFD-fed offspring of CON or CPS mothers. Those mice were placed under a 12-h LD cycle for 7 days and subsequently transferred to constant darkness. Actograms were double-plotted, showing 2 successive days for visualization. Dark phase is shadowed. Scale bar, 25 counts. (T) Free-running period of HFD-fed offspring mice of the CON and CPS mothers (n=3 animals per group). (U, V) Expression profiles of core clock and metabolic genes in the liver (U) and WAT (V). Transcripts were normalized to 18S rRNA (n=3-6 replicates per time points). ZT0 and ZT24 are double plotted for visualization. (W) Quantitation of the blot density of the hypothalamic proteins (n=3 replicates per time point per group). ZT0 and ZT24 are double plotted for visualization. (X, Y) Expression of metabolic genes in the skeletal muscle (X) and

brown adipose tissue (BAT, Y) at ZT12. Transcripts were normalized to 18S rRNA (n=4-5 replicates per time points).
*p<0.05, **p<0.01, ***p<0.001, and ****p<0.0001 by two-way ANOVA (vs CON(HFD), A, E-G, I, K-M, O-P, R, U). Data are presented as mean + SEM.

Figure S2. Offspring of the mothers devoid of *Bmal1* during pregnancy displays exacerbation of diet-induced obesity, related to Figure 2.
(A) Gene expression of the maternal liver following tamoxifen treatment and weaning of offspring mice. Transcripts were normalized to 18S rRNA (n=5 replicates per group). (B) BMAL1 protein in various tissues from wild-type and tamoxifen-inducible *Bmal1* knockout mothers. (C) Body mass index (BMI) determined by the bioimpedance method (n=5 animals per group). (D, E) Representative images of the liver (D) and WAT H&E staining (E). (F) Percentage of oil red O staining-positive areas shown in Figure 2G (n=3 mice per group, four areas were captured and analyzed in each mouse). (G) Percentage of F4/80 positive cells in the immunohistochemistry staining shown in Figure 2H. (H) Adipocyte size in H&E staining (areas of 50 cells derived from n=3 replicates per group (17, 17, 16 cells from each replicate) were counted in each group). (I) Percentage of extracellular fluid (top) and total body water (bottom) determined by the bioimpedance method (n=5 animals per group). (J) Serum levels of total cholesterol (left) and triglyceride (right) (WT: n=4; BKO: n=5). (K) Daily water intake (n=5 animals per group) in male offspring. L, light; D, dark. (L) Body weight of the LFD- or HFD-fed female offspring mice of the WT and BKO mothers (n=5 animals per group) and a representative image of the HFD-fed offspring mice of the WT and BKO mothers. (M) Representative photograph of the white adipose tissue (WAT) and liver from the HFD-fed female offspring mice of the WT and BKO mothers (top), and tissue weights of the LFD- or HFD-fed offspring mice of the WT and BKO mothers (n=5 tissues per group, bottom). peri, perirenal; para, parametrial; sub, subcutaneous. (N) Intraperitoneal glucose (top) and insulin tolerance tests (bottom) (n=5 animals per group). (O) Area under the curve (AUC) of the glucose (top) and insulin tolerance tests (bottom) (n=5 animals per group). (P) Metabolic cage assessment of the oxygen consumption (VO_2), energy expenditure, respiratory quotient (RQ), and carbon dioxide production (VCO_2) (n=4 animals per group) in female offspring mice aged from 14 to 16 weeks. (Q) Daily food intake and food intake adjusted by body weight (n=5 animals per group) in female offspring. L, light; D, dark. (R) Daily water intake (n=5 animals per group) in female offspring. L, light; D, dark. (S) Body mass index (BMI), percentage of fat mass, percentage of extracellular fluid and total body water determined using the bioimpedance method (n=5 animals per group). (T, U) Expression profiles of core clock genes at ZT12 in the liver (T) and WAT (U). Transcripts were normalized to 18S rRNA (n=5 replicates per group).
Data are presented as mean + SEM. *p<0.05, ***p<0.001, and ****p<0.0001 by student's *t* test (A, C, F-H, J) or by two-way ANOVA (K-Q, S). The ns denotes not significant.

Figure S3. Hepatic metabolome reveals temporal metabolic rewiring by maternal circadian disruption during pregnancy, related to Figure 3 and Table S1.
(A) Heat maps illustrating diurnal metabolites oscillating commonly in all 4 groups, CON, CPS conditions (n=5 per timepoint per group). (B) Number of rhythmic metabolites in each super-pathway. (C) Distribution of amplitude in hepatic metabolites commonly oscillating in all 4 groups. (D) Polar histograms showing the peak phase distribution of metabolites commonly rhythmic in all 4 groups. (E) Sub-pathway analysis on diurnal metabolites oscillating commonly in all 4 groups, CON, and CPS conditions. (F) Integrative analysis of enrichment and pathway topology on diurnal metabolites commonly in all 4 groups, CON, and CPS conditions. (G) Representative profiles of hepatic metabolites cycling commonly in all 4 groups (corticosterone), CON (gamma-glutamylphenylalanine), and CPS (ergothioneine) conditions. Data were presented as mean + SEM (n=5 biological replicates per time point per group). ZT0 and ZT24 are double plotted for visualization. (H) Integrative analysis of enrichment and pathway topology on diurnal metabolites in each group. (I) The hepatic pathway enrichment comparing the HFD-fed offspring born to the CON and CPS mothers at ZT0, ZT6, ZT12, and ZT18.

Figure S4. Maternal circadian disruption during pregnancy modulates hepatic circadian reprogramming by HFD, related to Figure 4 and Tables S2-3.
(A) Heat maps illustrating diurnal transcripts oscillating commonly in all 4 groups, CON, and CPS conditions (n=3 per timepoint per group). (B) Polar histograms showing the peak phase distribution of transcripts commonly rhythmic in all 4 groups. (C) Distribution of amplitude in hepatic transcripts commonly oscillating in all 4 groups. (D) GO terms of biological processes enriched in diurnal transcripts oscillating commonly in all 4 groups, CON, and CPS conditions. (E) Representative profiles of hepatic genes oscillating commonly in all 4 groups (*Gys2*), CON (*Igip*), and CPS (*Cds2*) conditions. Data were presented as mean + SEM (n=3 biological replicates per time point per group). ZT0 and ZT24 are double plotted for visualization. (F) Heat map illustrating differentially expressed genes in the liver between the HFD-fed offspring born to the CON and CPS mothers (n=3 per timepoint per group). (G) GO terms of biological processes enriched in differentially expressed genes in the liver between the HFD-fed offspring born to the CON and CPS mothers. (H) Principal Component Analysis of fecal microbiome of the LFD- or HFD-fed offspring mice of the WT and BKO mothers (n=5 per timepoint per group). (I) Breakdown of the microbial species of the LFD- or HFD-fed offspring mice of the WT and BKO mothers. (J) Alpha diversity assessed by Shannon and ACE indices. Data were presented as mean + SEM (n=5 per timepoint per group). (K) Beta diversity at the genus level determined by the Bray-Curtis index and principal coordinate analysis (PCoA) (n=5 per timepoint per group). (L) Pairwise PERMANOVA based on Bray-Curtis dissimilarity (n=5 per timepoint per group).

Figure S5. Maternal circadian disruption impacts fetal hepatic rhythmic gene expression, related to Figure 5.

(A) Daily food and water intake of CON and CPS conditions (n=4-5 animals per group, top), and of WT and BKO mice (n=4 animals per group, bottom) during pregnancy. (B) Breakdown of daily food and water intake of CON and CPS conditions in light and dark phases (n=4-5 animals per group, top), and of WT and BKO mice in subjective day and night (n=4 animals per group, bottom) during pregnancy. L, light; D, dark; SD, subjective day; SN, subjective night. (C) Number of fetuses of CON and CPS conditions (CON: n=20 samples; CPS: n=18 samples, top), and of WT and BKO mice (n=5 animals per group, bottom) on E18.5. (D) Weight of body, brain, heart, and kidney of fetus of CON and CPS mothers (n=5-8 samples per group, top), and of WT and BKO mothers (n=5-7 animals per group, bottom) on E18.5. (E) Expression of genes encoding hepatocyte-lineage markers in the fetal liver. Transcripts were normalized to 18S rRNA (n=3-5 replicates per time point per group). ZT0 and ZT24 are double plotted for visualization. (F, G) Expression of core clock genes in the maternal (F) and fetal (G) liver. Transcripts were normalized to 18S rRNA (n=4-5 (F), and n=3-5 (G) replicates per time point per group). ZT0 and ZT24 are double plotted for visualization. Dotted lines indicate peak phases determined by Cosinor analysis. (H) Correlation scatter plot showing the level of methylation at common CpG sites. Histograms of the percent methylation per sample and the Pearson correlation coefficients for each comparison are also shown. MCO denotes mouse CON; MPS, mouse CPS; FCO, fetus CON; FPS, fetus CPS. (I) Clustering dendrogram of CpG methylation of the CON and CPS livers from fetal and four-week-old offspring mice. (J) Pregnancy duration of the mothers exposed to either CON or CPS condition before pregnancy (CPS-BP) (n=5 animals per group). (K) Number of fetuses of CON and CPS-BP conditions (n=5 animals per group) on E18.5. (L) Representative images of the fetuses born to the CON and CPS-BP mothers. (M) Weight of body, liver, brain, heart, and kidney of fetus of CON and CPS-BP mothers (n=12 samples per group) on E18.5. (N) Pregnancy duration of the mothers exposed to either CON or CPS condition for two-thirds of pregnancy (2/3CPS) (n=5 animals per group). (O) Number of fetuses of CON and 2/3CPS conditions (n=5 animals per group) on E18.5. (P) Representative images of the fetuses born to the CON and 2/3CPS mothers. (Q) Weight of body, liver, brain, heart, and kidney of fetus of CON and 2/3CPS mothers (n=12 samples per group) on E18.5.

Data are presented as mean + SEM (A-B, D-G, M, Q), and ± SEM (C, J-K, N-O). *p<0.05, **p<0.01, and ****p<0.0001 by student's *t* test (A, D), or by two-way ANOVA (B, F-G) . The ns denotes not significant by student's *t* test (A, C-D, J-K, M-O, Q) or by two-way ANOVA (B).

Figure S6. Maternal circadian disruption impacts placental genomic signature, related to Figure 6.

(A) Expression profiles of *Slc38a4*, core clock and *Nampt* genes in the placenta. Transcripts were normalized to 18S rRNA and presented as mean + SEM (n=4-5 replicates per time point per group). ZT0 and ZT24 are double plotted for visualization. (B) Placental weight in CON and CPS condition before pregnancy (CPS-BP) on E18.5 day (n=12 replicates per group). (C) The ratio of fetal body weight (BW) to placental weight (PW) in CON and CPS-BP conditions (n=12) on E18.5 day. (D) Placental weight in CON and CPS condition for two-thirds of pregnancy (2/3CPS) on E18.5 day (n=12 replicates per group). (E) The ratio of fetal BW to PW in CON and 2/3CPS conditions (n=12) on E18.5 day. (F) Fractions of clusters in each sample. (G) UMAP visualization of placental cells colored by different clusters in each sample. (H) UMAP visualization of representative gene expression. (I) Distribution of CON versus CPS cells on UMAP plot (upper panels), and clustering of CON and CPS cells on UMAP plot (lower panels). SynT, Syncytiotrophoblast; S-TGC, Sinusoidal trophoblast giant cells; SpT, Spongiotrophoblast; GC, Glycogen cells. (J) GO terms of biological processes enriched in the endothelial cells (upper panels), blood and immune cells subcluster 1 (middle panels), and blood and immune cells subcluster 2 (lower panels).

Data are presented as mean + SEM (A-E). The ns denotes not significant by student's *t* test (B-E).

Figure S7. Circadian alignment of caloric restriction, not time-restricted feeding alone, in adult offspring abolishes diet-induced obese phenotype of offspring caused by maternal circadian disruption, related to Figure 7.

(A, B) Body mass index (BMI, A) and percentage of fat mass (B) determined by the bioimpedance method (n=4-10 animals per group). (C) Percentage of extracellular fluid and total body water by body composition measurement machine (n=4-10 animals per group). (D) Daily water intake separated by day and night (n=3 animals per group). L, light; D, dark. (E) Adipocyte size in H&E staining (areas of 50 cells derived from n=3 replicates per group (17, 17, 16 cells from each replicate) were counted in each group). Data are presented as mean ± SEM. (F) Serum levels of total cholesterol (left) and triglyceride (right) (n=5 samples per group). (G) Expression profiles of clock genes in the liver. Transcripts were normalized to 18S rRNA and presented as mean + SEM (n=4-5 replicates per time point per group). (H, I) Expression profiles of clock genes (H), and metabolic genes (I) in the WAT. Transcripts were normalized to 18S rRNA and presented as mean + SEM (n=3-5 replicates per time point per group). (J) Body weight of the calorie-restricted, HFD-fed (HFD_CR) female offspring mice of the CON and CPS mothers (n=5 animals per group) and a representative image. (K) Body mass index (BMI) and percentage of fat mass determined using the bioimpedance method (n=5 animals per group). (L) Representative photograph of the white adipose tissue (WAT) and liver from the HFD_CR female offspring mice of the

CON and CPS mothers (top), and tissue weights of the HFD_CR offspring mice of the CON and CPS mothers (n=5 tissues per group, bottom). peri, perirenal; para, parametria; sub, subcutaneous. (M) Intraperitoneal glucose tolerance test (IPGTT, top) and insulin tolerance test (IPITT, bottom) (n=5 animals per group). (N) Area under the curve (AUC) of IPGTT (top) and IPITT (bottom) (n=5 animals per group). (O) Metabolic cage assessment of oxygen consumption (VO_2, top) and energy expenditure (bottom) (n=4 animals per group) in female offspring mice aged 14 to 16 weeks. (P) Metabolic cage assessment of the respiratory quotient (RQ, top) and carbon dioxide production (VCO_2, bottom) (n=4 animals per group) in female offspring mice aged 14 to 16 weeks. (Q) Daily food intake adjusted based on body weight (n=5 animals per group). (R) Daily water intake (n=5 animals per group). L, light; D, dark. (S) Percentage of extracellular fluid and total body water determined by the bioimpedance method (n=5 animals per group).

*p<0.05, **p<0.01, ***p<0.001, and ****p<0.0001 by two-way ANOVA (A, E-G, I). The ns denotes not significant. Data are presented as mean + SEM (A-D, F-S).